Università
degli Studi
di Ferrara

Dipartimento
di Fisica
e Scienze della Terra

Geoneutrinos from Potassium in the Earth

Advisor:
Prof. Fabio Mantovani

Co-Advisor:
Dott.sa Marica Baldoncini
Dott.sa Virginia Strati

Graduating:
Andrea Serafini

Academic Year 2017-2018

Outline

- Earth formation and evolution: open questions
- A probe to investigate Earth interior: geoneutrinos
- ^{40}K geoneutrino detection: challenges and strategies
- Study of target nuclei for ^{40}K geoneutrino detection through Inverse Beta Decay (IBD)
- Estimation of ^{40}K geoneutrino signal

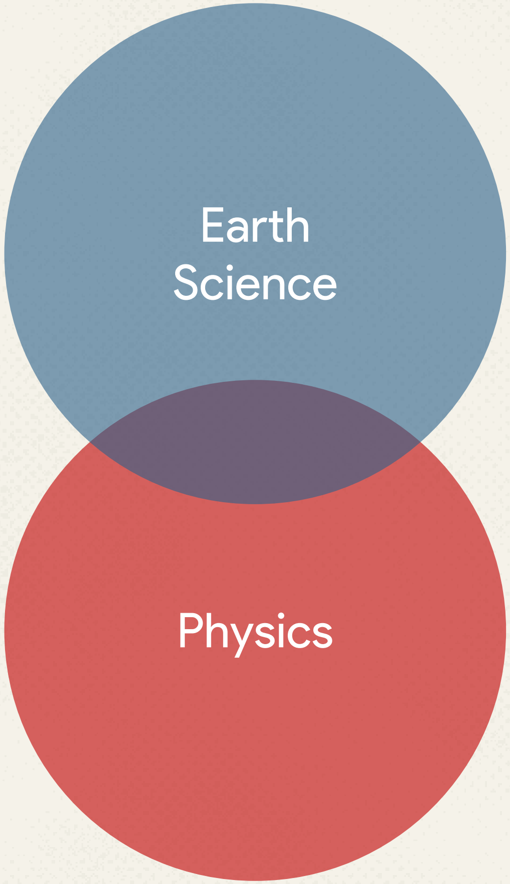

Scientific motivations

Earth is mainly **inaccessible**: we cannot directly access its interior.
What we actually know comes from:

- **seismological** reconstruction of density profile and **geophysical** features throughout all Earth
- **rock samples** from the Crust (and the upper portion of the Mantle), useful for **geochemical** analysis.

Typically, assumptions on which **building blocks** have been used to form our planet Earth in the beginning are inferred from meteorites:

Enstatites Chondrites

Carbonaceous Chondrites

These are characterized by completely different elemental abundances.

Knowing **Earth composition** would permit to better understand the **processes** that lead our planet to be what it is now.

Earth evolution

Earth evolution

1st differentiation

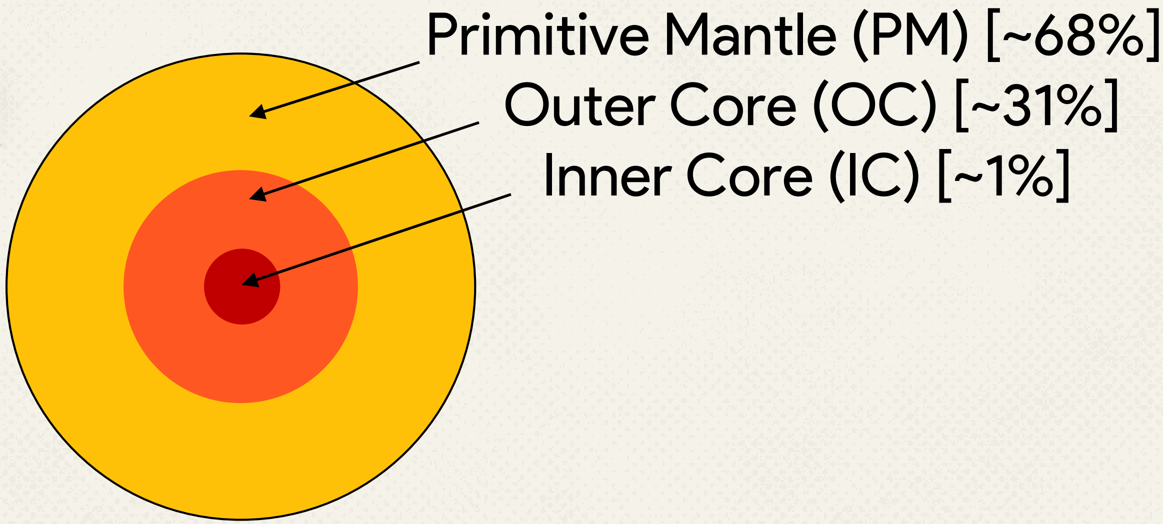

Siderophile elements (+Fe) in the Core

Earth evolution

1st differentiation

Primitive Mantle (PM) [~68%]
Outer Core (OC) [~31%]
Inner Core (IC) [~1%]

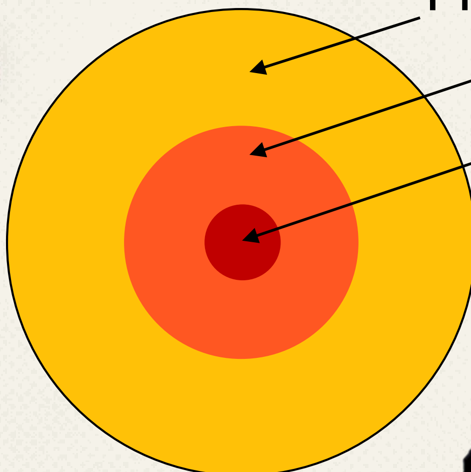

Siderophile elements (+Fe)
in the Core

2nd differentiation

Lithosphere [~2%]
Mantle [~66%]
OC+IC [~32%]

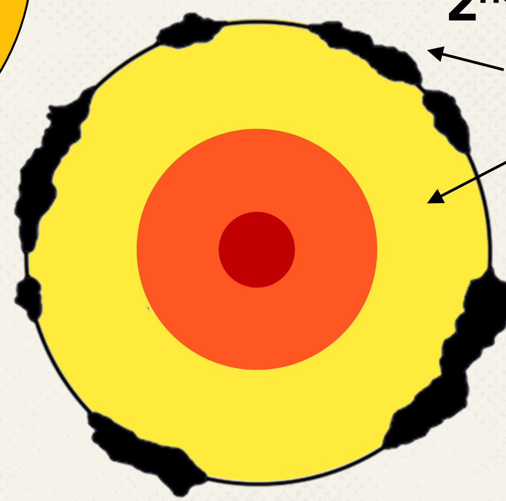

Lithophile elements (+O)
in the Lithosphere (e.g. U, Th, K)

Earth evolution

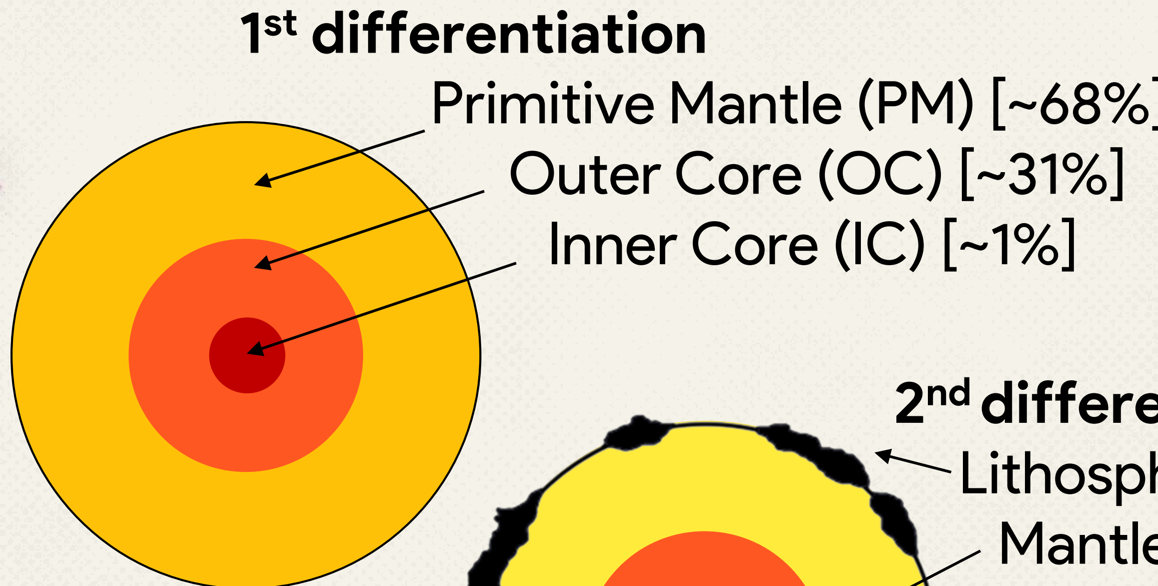

Siderophile elements (+Fe) in the Core

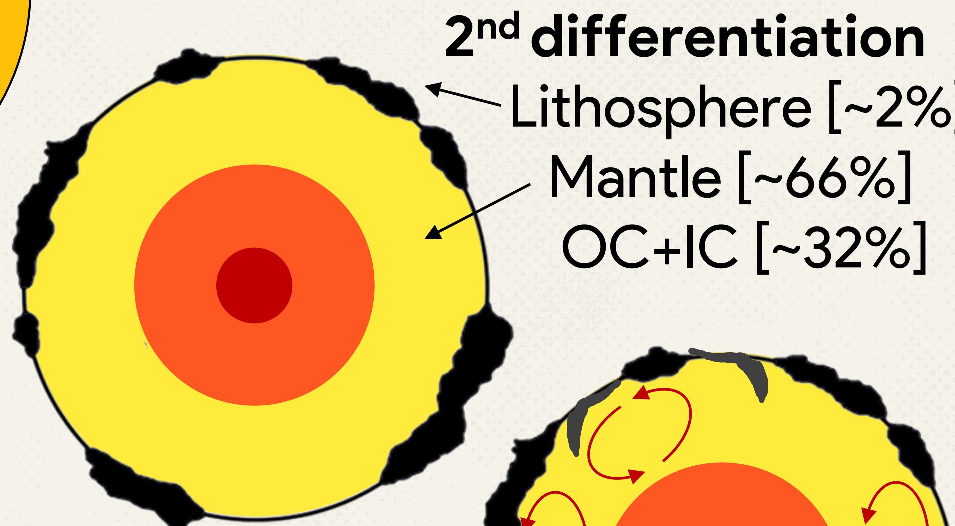

Lithophile elements (+O) in the Lithosphere (e.g. U, Th, K)

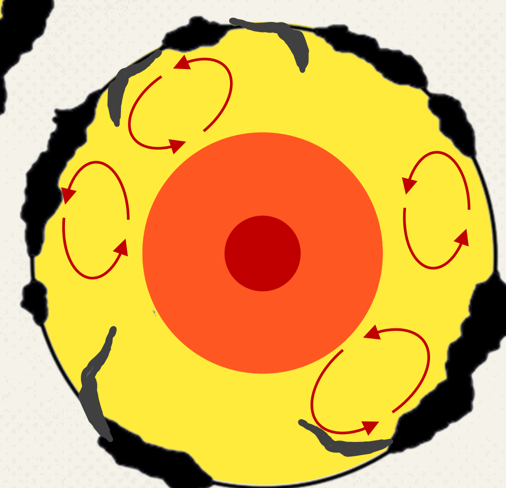

Convective and tectonic processes: formation of new crust (oceanic crust) and recycling of continental crust (up to 10 times)

A Standard Model of the Earth

Earth has a well established **layered** structure, visible from its **density profile**:

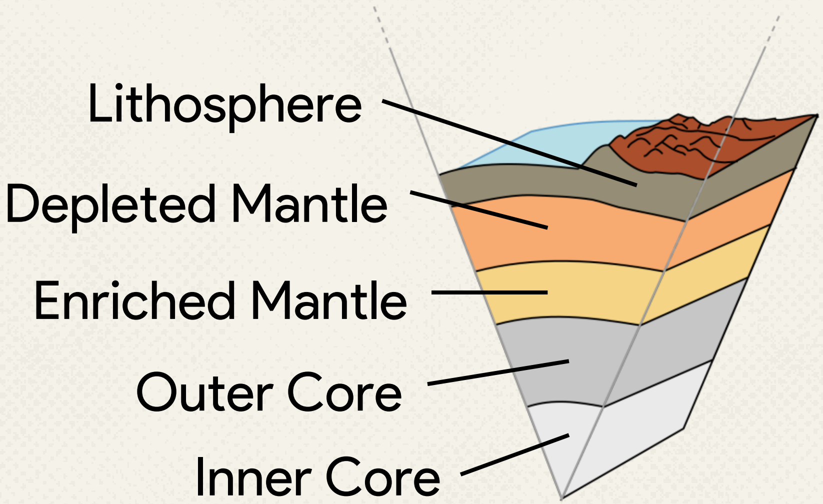

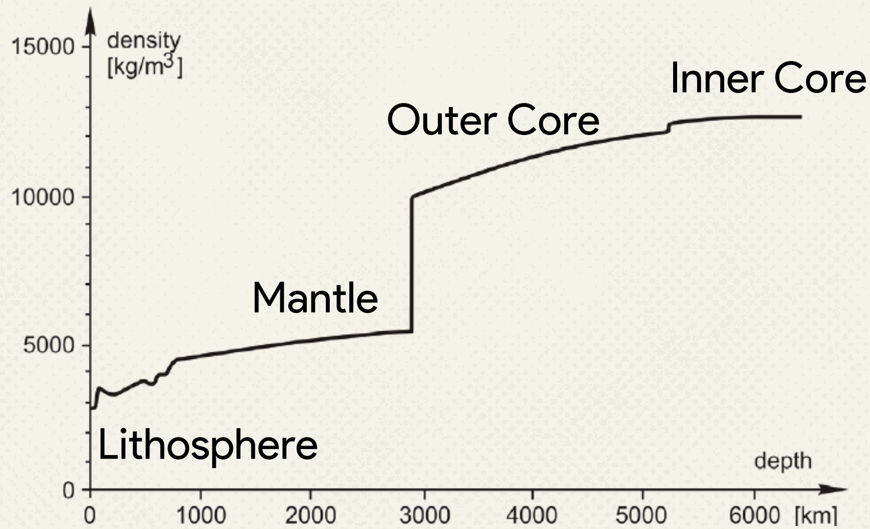

A Standard Model of the Earth

Earth has a well established **layered** structure, visible from its **density profile**:

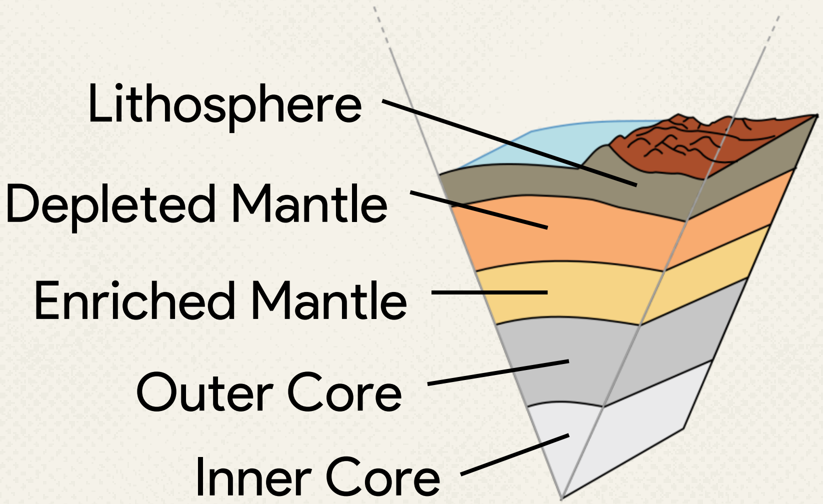

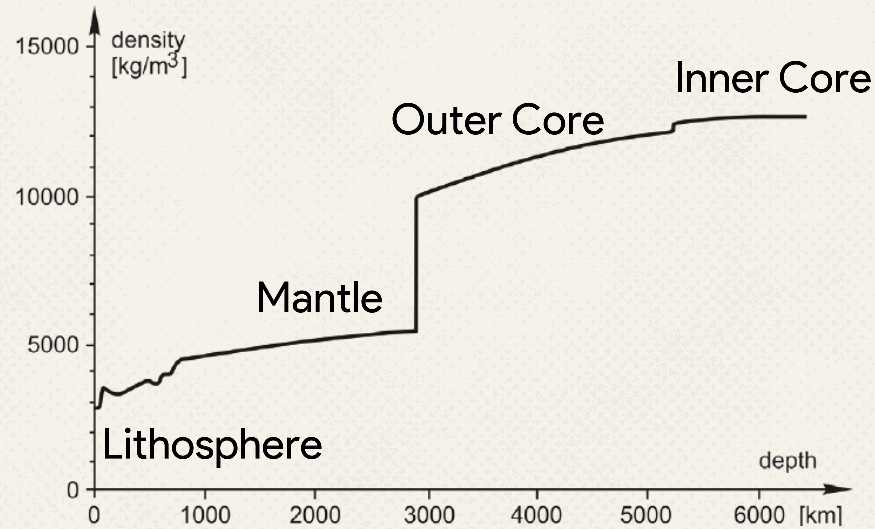

Bulk Earth's mass composition	
Iron (Fe)	32%
Oxygen (O)	30%
Silicon (Si)	16%
Magnesium (Mg)	15%

About 0.02% of Earth's mass is made out of radioactive **Heat Producing Elements (HPEs)**.

The most important for activity, abundances and half-life time (comparable to Earth's age) are:

- **Uranium U** (~10^{-8} M_{Earth})
- **Thorium Th** (~10^{-7} M_{Earth})
- **Potassium K** (~10^{-4} M_{Earth})

The main reservoirs of the Earth

Despite Earth's structure is well understood, its chemical composition is not. Only for Lithosphere a coherent statistical study can be performed on samples.

Lithosphere rich in HPEs, directly measurable.

Mantle inaccessible to direct measurements.

Core inaccessible and void of HPEs

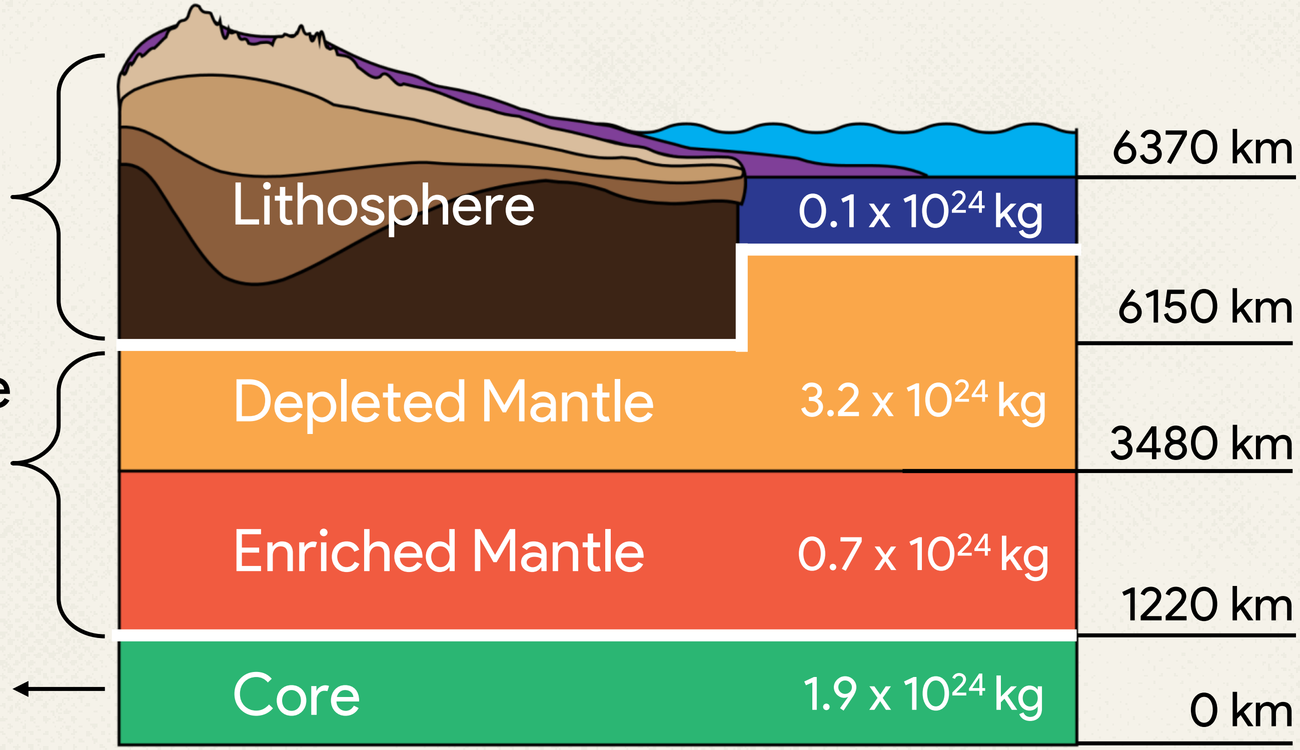

	a(U) [μg/g]	a(Th) [μg/g]	a(K) [10^{-2}g/g]
Lithosphere	$0.25^{+0.07}_{-0.06}$	$1.08^{+0.37}_{-0.23}$	$0.28^{+0.07}_{-0.06}$
Depleted Mantle	?	?	?
Enriched Mantle	?	?	?

Bulk Silicate Earth (BSE) Models

The Primitive Mantle's composition is described by the paradigm of the BSE.

Among the several models proposed, these are the ones predicting the **minimum**, the **standard** and the **maximum** values for HPEs' masses

Cosmochemical Model (CCM)

- Enstatitic composition

- Low HPEs content

Geochemical Model (GCM)

- Carbonaceous composition

- Medium HPEs content

Geodynamical Model (GDM)

- Based on Earth dynamics
- High HPEs content

	CCM	GCM	GDM
M(U) *[10^{16} kg]*	*4.8*	*8.1*	*14.1*
M(Th) *[10^{16} kg]*	*17.4*	*32.3*	*56.5*
M(K) *[10^{19} kg]*	***58.9***	***113.0***	***141.2***

The typical uncertainties of individual models are typically ~20%, of second order compared to a factor ~3 variability among models.

Earth scenarios for geoneutrinos

Not only HPEs' content, but also their distribution inside the Earth is not fully known.

Taking into account geophysical, geochemical and cosmochemical constraints, we built three (**Low**, **Standard** and **High**) scenarios which embrace the maximum HPE's contents variability.

For each HPE: $$M_{mantle} = M_{BSE} - M_{litho}$$

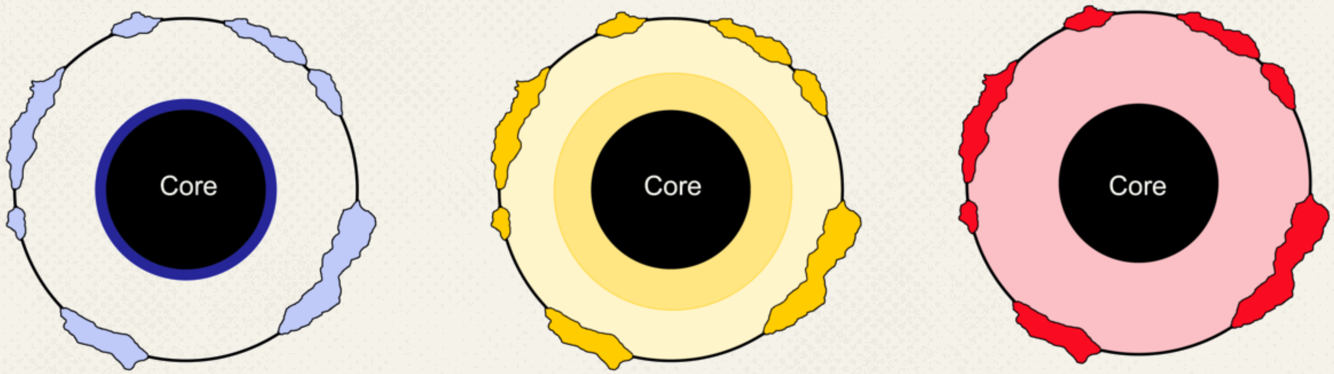

	Low Scenario	Standard Scenario	High Scenario
M_{BSE}	M_{CCM}	M_{GCM}	M_{GDM}
M_{litho}	$M_{Std} - 1\sigma$	M_{Std}	$M_{Std} + 1\sigma$
M_{mantle}	0	$0.62 \cdot (M_{GCM} - M_{Std})$	$M_{GDM} - (M_{Std} + 1\sigma)$
	$M_{CCM} - (M_{Std} - 1\sigma)$	$0.38 \cdot (M_{GCM} - M_{Std})$	

Geoneutrinos: main physical properties

- Geoneutrinos are $\bar{\nu}_e$ produced in naturally occurring β^- decays of HPEs in the Earth.
- $\varepsilon(\bar{\nu})$ provides the $\bar{\nu}_e$ production rate for kg of the HPE.
- They can cross the entire planet **almost without interacting**, bringing instantaneous information on the Earth's composition.
- Geo-$\bar{\nu}_e$ from **^{40}K** could represent an important tool thanks to their **higher luminosity**.

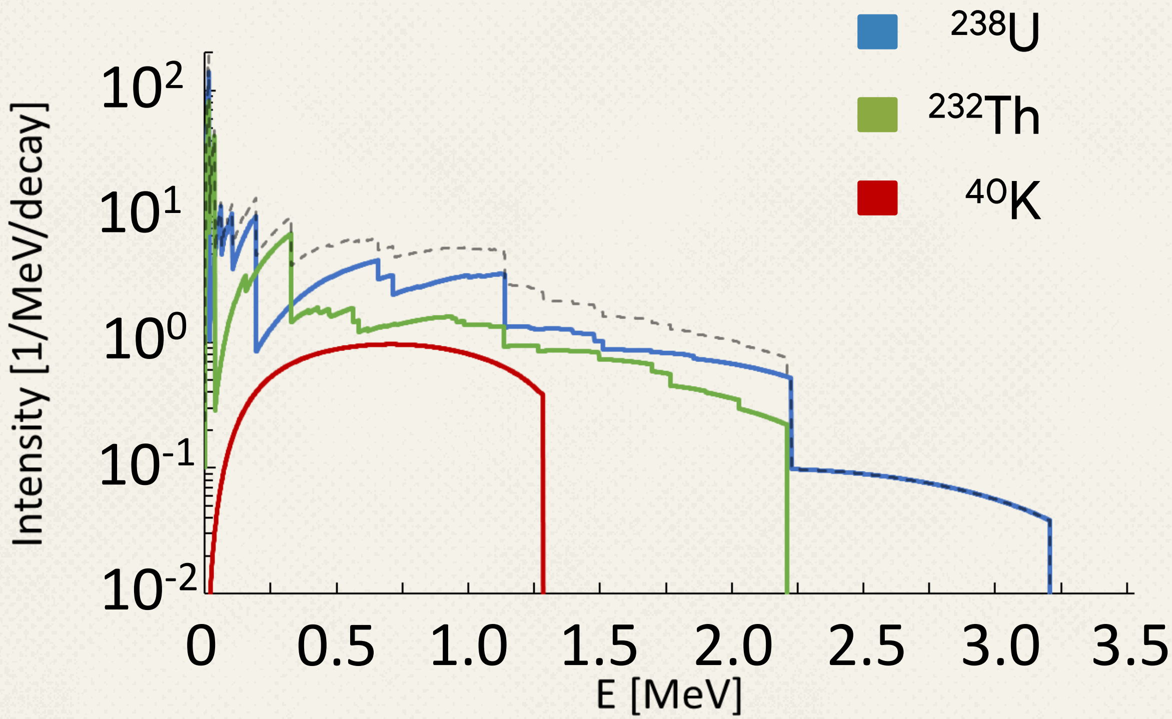

Decay	$T_{1/2}$ [10^9 y]	$\varepsilon(\bar{\nu})$ [10^7 kg^{-1} s^{-1}]	$E_{max}(\bar{\nu})$ [MeV]
$^{238}U \rightarrow {}^{206}Pb + 8\alpha + 6\beta^-$	4.47	7.5	3.36
$^{232}Th \rightarrow {}^{208}Pb + 6\alpha + 4\beta^-$	14.0	1.6	2.25
$^{40}K \rightarrow {}^{40}Ca + e^- + \bar{\nu}_e$ (89%)	1.28	**23.2**	1.31

Inverse Beta Decay (IBD) detection

Geoneutrinos are **detected by IBD** in ***~kton*** Liquid Scintillation Detectors.

$$\bar{\nu}_e + p \rightarrow n + e^+ - 1.806\ MeV$$

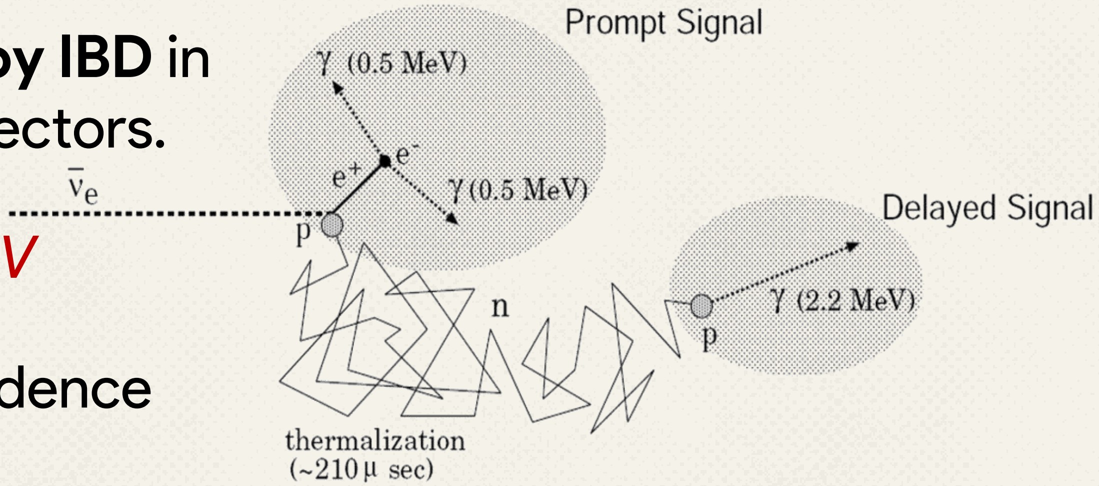

Detection requires the coincidence of 2 delayed light signals.

It does not permit to observe ^{40}K-$\bar{\nu}_e$

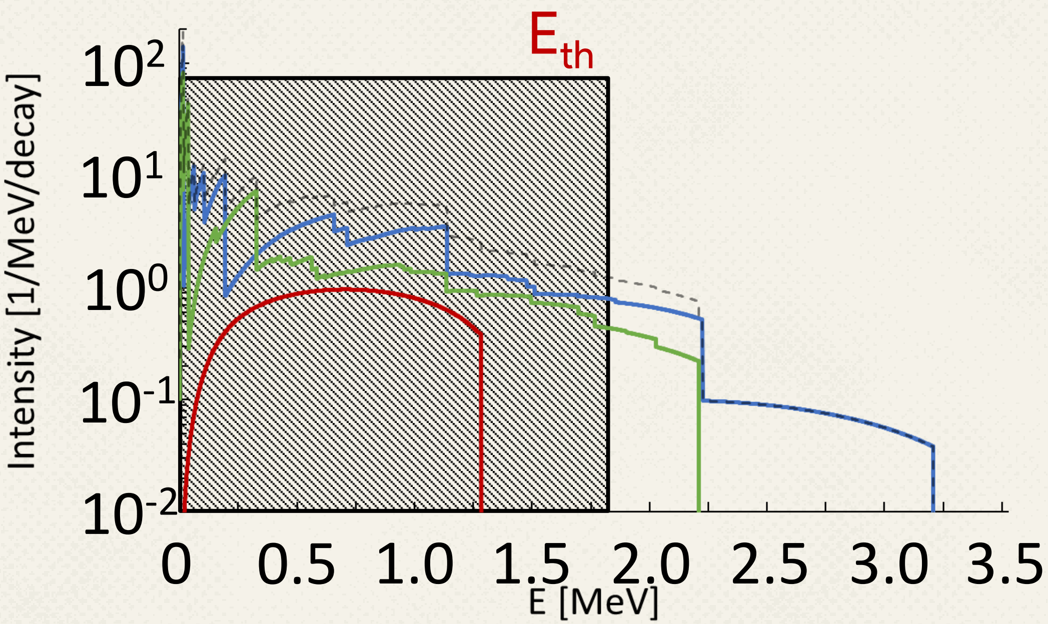

Inverse Beta Decay (IBD) detection

Geoneutrinos are **detected by IBD** in ***~kton*** Liquid Scintillation Detectors.

$$\bar{\nu}_e + p \rightarrow n + e^+ - 1.806\ MeV$$

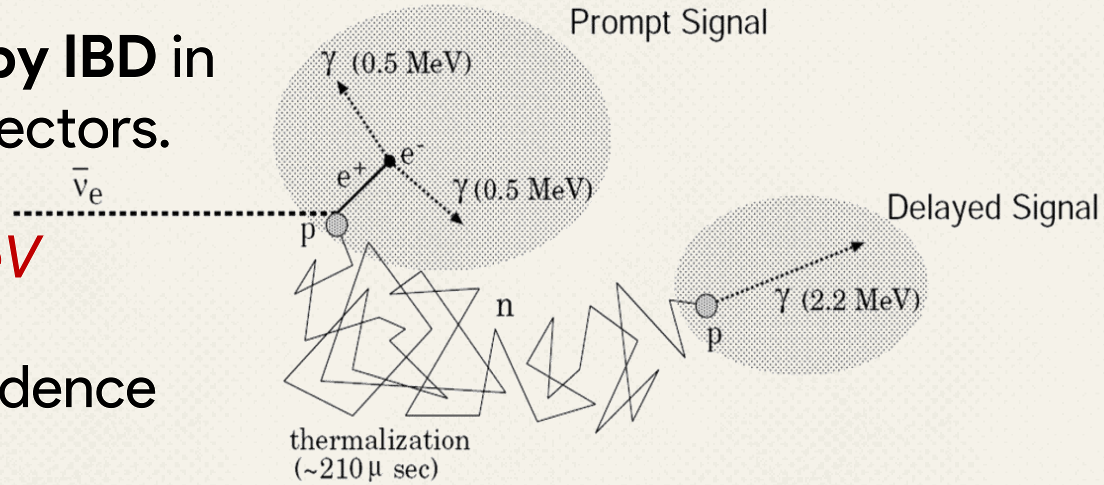

Detection requires the coincidence of 2 delayed light signals.

It does not permit to observe ^{40}K-$\bar{\nu}_e$

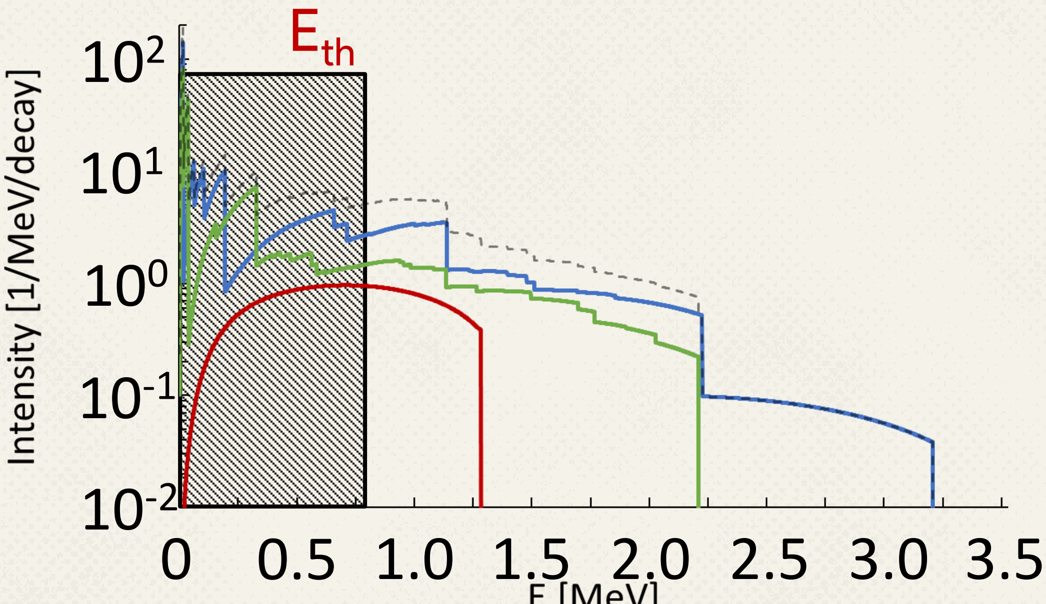

In order to detect ^{40}K- $\bar{\nu}_e$ we could use:

$$\bar{\nu}_e + {}_{Z+1}^{A}Y \rightarrow {}_{Z}^{A}X + e^+ - E_{th}$$

We shall require:

- $E_{th} < 1.3\ MeV$
- High cross-section
- High Y natural isotopic abundance

Geoneutrino signal ingredients

The geoneutrino signal evaluation requires several ingredients for modeling the three geoneutrino life stages:

- **production** inside the Earth
- **propagation** to the detector site
- **detection** in liquid scintillation detectors

$$S_{i,n} \propto Sp_i(E) \otimes \Phi_i(m,\vec{r}) \otimes P_{ee}(E,\vec{r}) \otimes \sigma_n(E) \otimes N_{target,n} \otimes T$$

Nuclear

- $Sp_i(E)$ = $\bar{\nu}_e$ emission spectra where i = ^{238}U, ^{232}Th, ^{40}K

Geology

- $\Phi_i(m_i,\vec{r})$ = unoscillated $\bar{\nu}$ flux at surface, where m_i is the mass of the *i-th* HPE placed at a distance $\vec{r}$ from the detector

Detector

- $N_{target,\,n}$= number of target nuclei where n runs over the IBD target candidates
- T = acquisition time

ν phisics

- $P_{ee}(E,\vec{r})$ = $\bar{\nu}_e$ survival probability
  $\langle P_{ee}\rangle$ = 0.55 for $|\vec{r}|$>50 km
- $\sigma_n(E)$ = IBD cross-section on nucleus target n

IBD Cross-sections

$$\sigma(E) = \frac{{G_F}^2}{\pi} \cos^2\theta_C \left|M_{fi}\right|^2 p\, E\, F(Z,E)$$

$\begin{pmatrix} c = 1 \\ \hbar = 1 \end{pmatrix}$

Nuclear Physics

- G_F = Fermi constant
- θ_C = 13.02° Cabibbo angle
- $\left|M_{fi}\right|^2$ = Squared Matrix element $\propto \frac{1}{ft}$
- ft = Comparative half-life
- *F(Z,E)* = Fermi nuclear function

$\bar{\nu}_e$ Kinematics

- p = $\bar{\nu}_e$ momentum
- E = $\bar{\nu}_e$ energy

After a first steep rise dominated by the Fermi Function *F(Z,E)* the cross-section increases as:

$$\sigma_n(E) \propto E^2$$

Different nuclei differ only for:

- E_{th} energy threshold
- *F(Z,E)* Fermi Function
- *ft* value

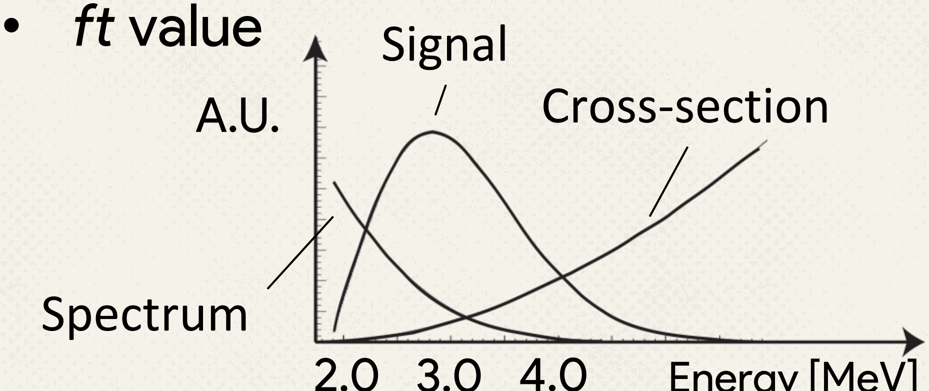

Candidate IBD target Isotopes

	Z	Isotopic abundance	E_{th} [MeV]	log ft
^{1}H	1	0.9999	1.806	3.0
^{3}He	2	1.34×10^{-6}	1.041	3.1
^{14}N	7	0.9964	1.178	9.0
^{35}Cl	17	0.7576	1.189	5.0
^{63}Cu	29	0.6915	1.089	6.7
^{79}Br	35	0.5069	1.268	4.7
^{106}Cd	48	0.0125	1.212	4.5

- For ^{3}He and ^{106}Cd, **isotopic abundances** precludes the construction of a *kton* detector
- ^{79}Br has a **small energy window** below the Potassium endpoint
- ^{14}N and ^{63}Cu have **high *ft* values** → Low cross-section

Data taken from ENSDF database

Candidate IBD target Isotopes

	Z	Isotopic abundance	E_{th} [*MeV*]	log *ft*
^{1}H	1	0.9999	1.806	3.0
^{3}He	2	1.34×10^{-6}	1.041	3.1
^{14}N	7	0.9964	1.178	9.0
^{35}Cl	17	0.7576	1.189	5.0
^{63}Cu	29	0.6915	1.089	6.7
^{79}Br	35	0.5069	1.268	4.7
^{106}Cd	48	0.0125	1.212	4.5

- For ^{3}He and ^{106}Cd, **isotopic abundances** precludes the construction of a *kton* detector
- ^{79}Br has a **small energy window** below the Potassium endpoint
- ^{14}N and ^{63}Cu have **high *ft* values** → Low cross-section

Data taken from ENSDF database

Candidate IBD target Isotopes

	Z	Isotopic abundance	E_{th} [*MeV*]	log *ft*
^{1}H	1	0.9999	1.806	3.0
^{3}He	2	1.34×10^{-6}	1.041	3.1
^{14}N	7	0.9964	1.178	9.0
^{35}Cl	17	0.7576	1.189	5.0
^{63}Cu	29	0.6915	1.089	6.7
^{79}Br	35	0.5069	1.268	4.7
^{106}Cd	48	0.0125	1.212	4.5

- For ^{3}He and ^{106}Cd, **isotopic abundances** precludes the construction of a *kton* detector
- ^{79}Br has a **small energy window** below the Potassium endpoint
- ^{14}N and ^{63}Cu have **high *ft* values** → Low cross-section

Data taken from ENSDF database

Candidate IBD target Isotopes

	Z	Isotopic abundance	E_{th} [*MeV*]	log *ft*
^{1}H	1	0.9999	1.806	3.0
^{3}He	2	1.34×10^{-6}	1.041	3.1
^{14}N	7	0.9964	1.178	9.0
^{35}Cl	17	0.7576	1.189	5.0
^{63}Cu	29	0.6915	1.089	6.7
^{79}Br	35	0.5069	1.268	4.7
^{106}Cd	48	0.0125	1.212	4.5

- For ^{3}He and ^{106}Cd, **isotopic abundances** precludes the construction of a *kton* detector
- ^{79}Br has a **small energy window** below the Potassium endpoint
- ^{14}N and ^{63}Cu have **high *ft* values** → Low cross-section

Data taken from ENSDF database

IBD Cross-sections

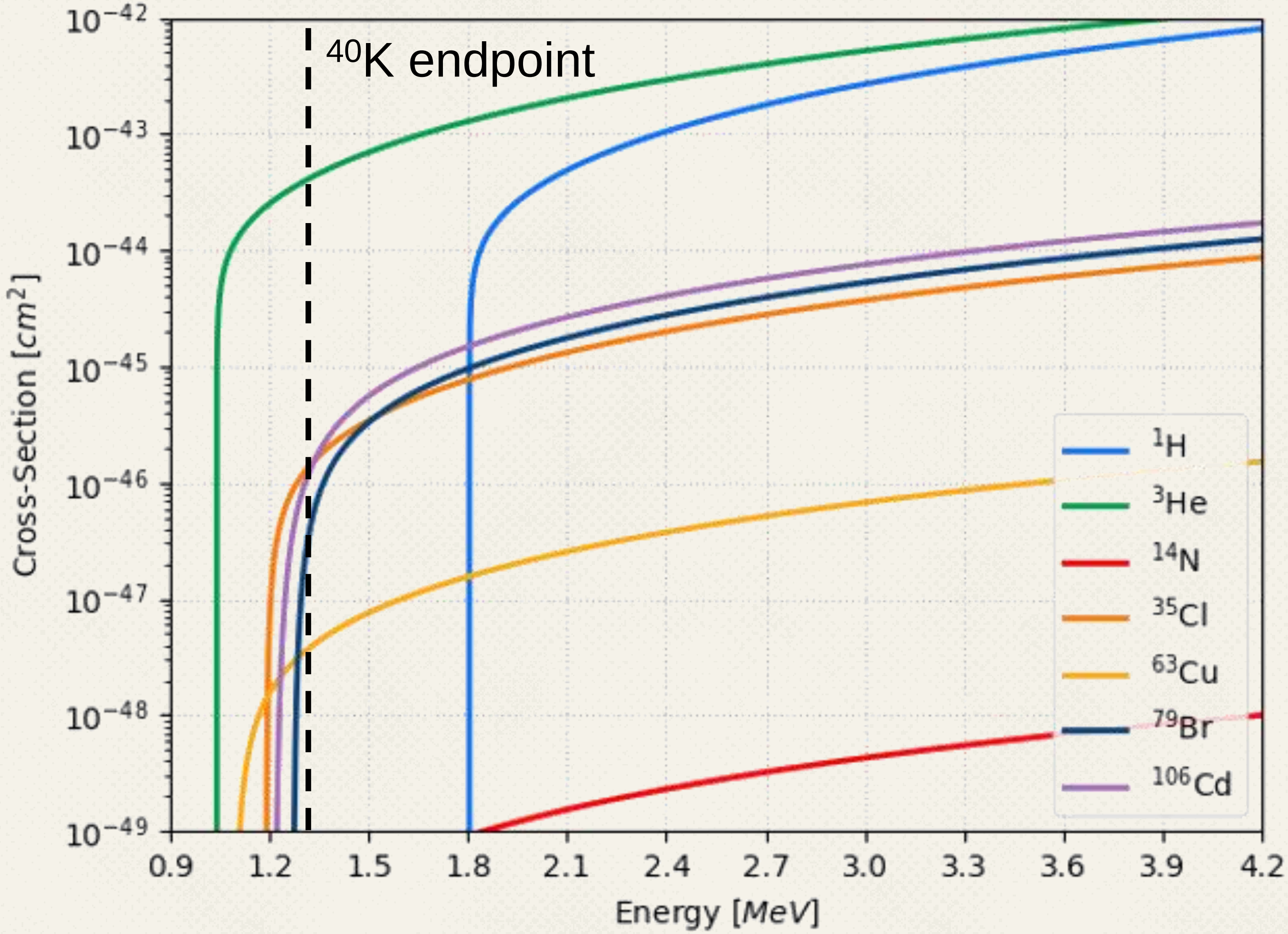

- Cross-sections for IBD on single target isotope in [cm^2]
- Estimated cross sections values span over **6 orders of magnitude.**
- The lowest threshold is 1.041 MeV for ^{3}He, the highest is 1.268 MeV for ^{79}Br

Weighted IBD Cross-sections

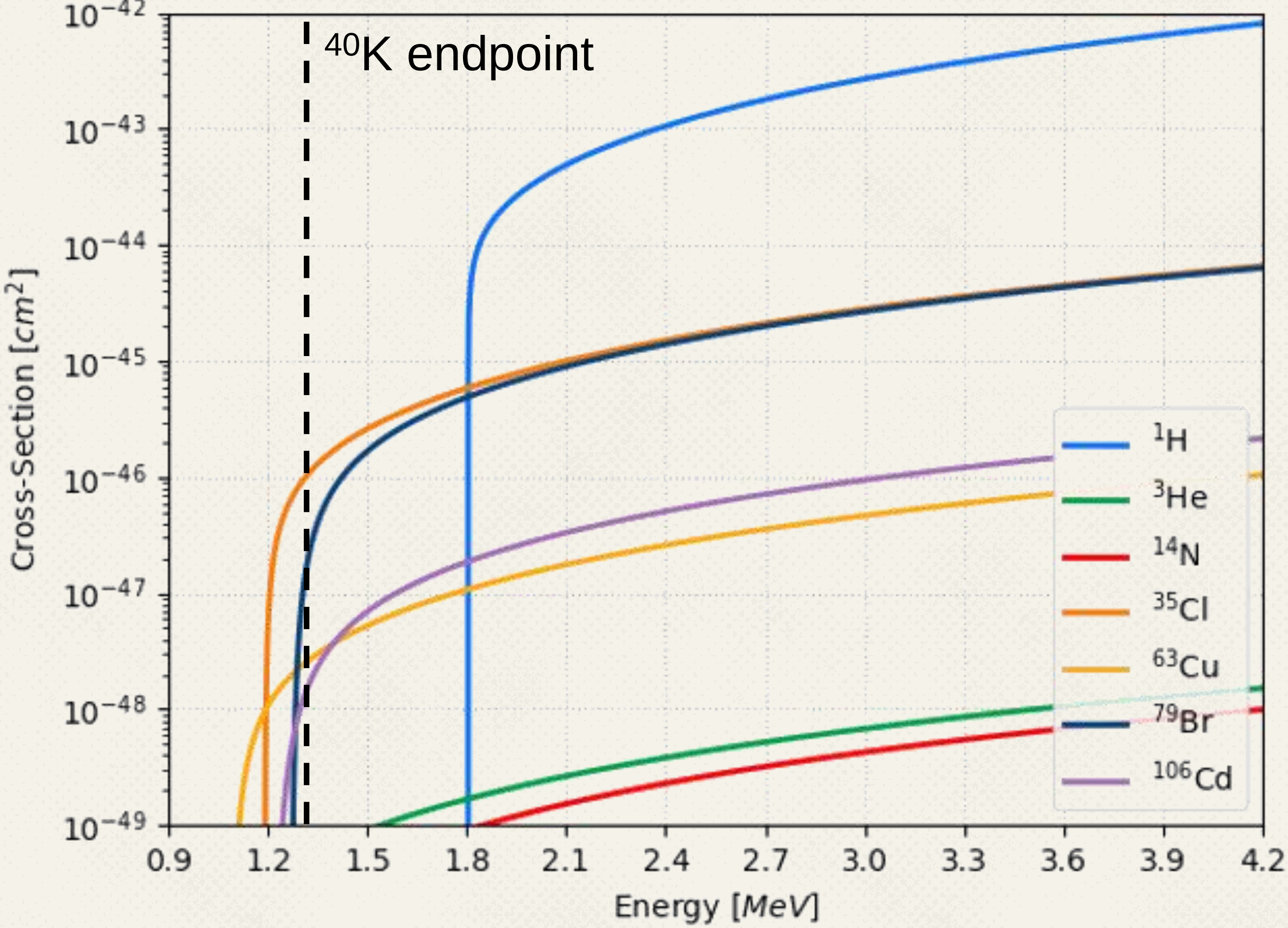

- **^{3}He**, which seemed the perfect candidate, is disfavored by its **abundance**
- **^{79}Br** has a 1.268 MeV **threshold, just** ***43 keV*** below the ^{40}K endpoint
- **^{35}Cl** has both a **low threshold** and a **good weighted cross-section**

Geoneutrino Signals

$$S_{i,n}(\vec{r}) = \frac{N_{target,n} \cdot T}{M_i \cdot \tau_i} \cdot \iint \frac{a_i(\vec{r}') \cdot \rho(\vec{r}')}{4\pi|\vec{r} - \vec{r}'|^2} \cdot P_{ee}(|\vec{r} - \vec{r}'|, E_\nu) \cdot Sp_i(E_\nu) \cdot \sigma_n(E_\nu)\, d^3r'\, dE_\nu$$

$n = {}^{1}H, {}^{3}He, {}^{14}N, {}^{35}Cl, {}^{63}Cu, {}^{79}Br, {}^{106}Cd$

$i = {}^{238}U, {}^{232}Th, {}^{40}K$

$N_{target,n}$	$10^{32} \cdot C_n$ with C_n isotopic ab.
T	1 year
M_i	Mass of i-th HPE atom
τ_i	Mean lifetime of i-th HPE
$a_i(\vec{r}')$	Abundance of i in $\vec{r}'$
$\rho(\vec{r}')$	Earth density
$P_{ee}(\|\vec{r} - \vec{r}'\|, E_\nu)$	Survival probability for $\bar{\nu}_e$
$Sp_i(E_\nu)$	$\bar{\nu}_e$ energy spectra for i-th HPE
$\sigma_n(E_\nu)$	IBD cross-section on atom n

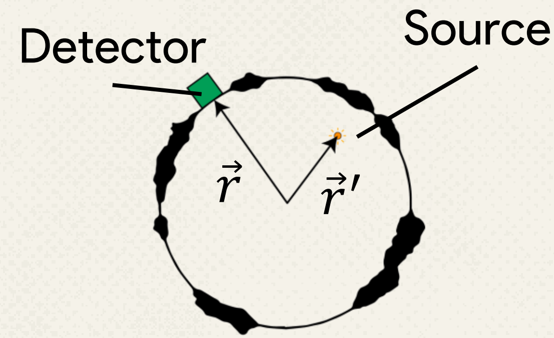

Geoneutrinos signals were evaluated at:

- Kamioka
- Gran Sasso
- Himalaya
- Hawaii

Signals and isotopes' hierarchy

For each site a signal variability range was estimated according to the **Low**, **Standard** and **High** Scenarios. S_{ref} [S_{low}, S_{high}].

Signal are expressed in TNU: events per 10^{32} targets per year

	S(^{40}K) [TNU]	
	Gran Sasso	**Kamioka**
^{35}Cl	**0.094 [0.061, 0.124]**	**0.070 [0.042, 0.092]**
^{63}Cu	4.40 [2.84, 5.80]× 10^{-3}	3.30 [1.99, 4.34]× 10^{-3}
^{79}Br	2.58 [1.66, 3.39]× 10^{-3}	1.93 [1.16, 2.54]× 10^{-3}
^{106}Cd	6.38 [4.12, 8.41]× 10^{-4}	4.78 [2.88, 6.30]× 10^{-4}
^{3}He	1.58 [1.02, 2.08]× 10^{-4}	1.18 [0.71, 1.56]× 10^{-4}
^{14}N	2.28 [1.47, 3.01]× 10^{-5}	1.71 [1.03, 2.25]× 10^{-5}

- To compare with S(U+Th)~10^1 TNU on ^{1}H
- ^{35}Cl is the best candidate for ^{40}K geo-$\bar{\nu}_e$ detection.
- The signal variability among the different scenarios is of a factor ~2

^{40}K Geoneutrino Signals at 4 sites

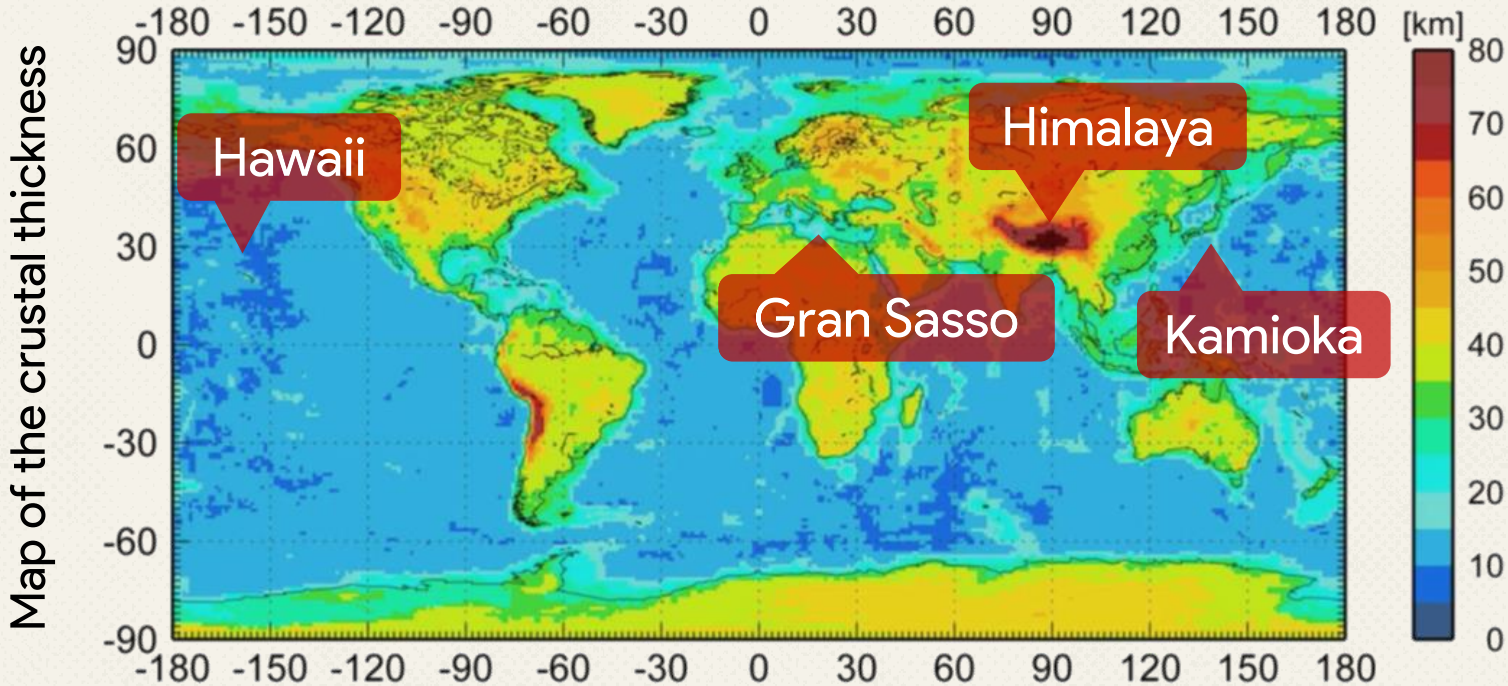

	Hawaii	Kamioka	Gran Sasso	Himalaya
S_{ref} [TNU] for ^{35}Cl	0.035	0.070	0.094	0.132
Lithosphere Mantle	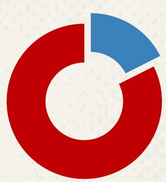	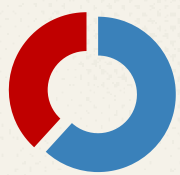	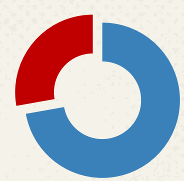	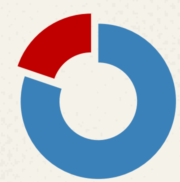

Hawaii has the lowest signal, with 83% coming from the Mantle.

Kamioka and Gran Sasso show comparable overall signals.

Himalaya has the highest signal, with 80% coming from the Lithosphere.

Conclusions and Perspectives

- **Three Earth scenarios** have been studied to predict the expected geo-$\bar{\nu}_e$ signal at surface, accounting for the **variability** of HPEs masses and distributions presented by different **BSE models.**
- Potassium $\bar{\nu}_e$ remains undetected. A list of **six candidate isotopes** (^{3}He,^{14}N,^{35}Cl,^{63}Cu,^{79}Br,^{106}Cd) suitable for **^{40}K-$\bar{\nu}_e$ IBD detection** has been found.
- IBD cross section has been calculated for each isotope candidate, with **^{35}Cl** resulting the **best option** in terms of expected signal.
- **Expected $\bar{\nu}_e$ signals** have been evaluated at **4** different **sites on Earth**, for each IBD isotope candidate.

Conclusions and Perspectives

- **Three Earth scenarios** have been studied to predict the expected geo-$\bar{\nu}_e$ signal at surface, accounting for the **variability** of HPEs masses and distributions presented by different **BSE models.**
- Potassium $\bar{\nu}_e$ remains undetected. A list of **six candidate isotopes** (^{3}He, ^{14}N, ^{35}Cl, ^{63}Cu, ^{79}Br, ^{106}Cd) suitable for **^{40}K-$\bar{\nu}_e$ IBD detection** has been found.
- IBD cross section has been calculated for each isotope candidate, with **^{35}Cl** resulting the **best option** in terms of expected signal.
- **Expected $\bar{\nu}_e$ signals** have been evaluated at **4** different **sites on Earth**, for each IBD isotope candidate.

Next steps:

- Study physical and **geological uncertainties** to provide a second order correction to these results.
- Evaluate the cost associated with each isotope to study the feasibility of a detector.

THAN^{40}KS FOR YOUR ATTENTION

BACK UP

Survival Probability

$$|\nu_i> = \sum_{\alpha=e,\mu,\tau} U_{\alpha,i} |\nu_\alpha>$$

Pontecorvo–Maki–Nakagawa–Sakata matrix

$$U = \begin{pmatrix} c_{12}c_{13} & s_{12}c_{13} & s_{13}e^{-i\delta} \\ -s_{12}c_{23} - c_{12}s_{23}s_{13}e^{i\delta} & c_{12}c_{23} - s_{12}s_{23}s_{13}e^{i\delta} & s_{23}c_{13} \\ s_{12}s_{23} - c_{12}c_{23}s_{13}e^{i\delta} & -c_{12}s_{23} - s_{12}c_{23}s_{13}e^{i\delta} & c_{23}c_{13} \end{pmatrix}$$

	Best fit	1σ range
δm^2	7.34×10^{-5} eV^2	$[7.20 – 7.51] \times 10^{-5}$ eV^2
$sin^2\theta_{12}$	3.04×10^{-1}	$[2.91 – 3.18] \times 10^{-1}$
$sin^2\theta_{13}$	2.14×10^{-2}	$[2.07 – 2.23] \times 10^{-2}$
$\|\Delta m^2\|$	2.455×10^{-3} eV^2	$[2.423 – 2.490] \times 10^{-3}$ eV^2
$sin^2\theta_{23}$	5.51×10^{-1}	$[4.81 – 5.70] \times 10^{-1}$
δ	1.32 π	[1.14 π – 1.55 π]

$$P_{e\to e}(E,L) \sim cos^4\theta_{13}\left(1 - sin^2 2\theta_{12} sin^2\left(\frac{\delta m^2 L}{4E}\right)\right) + sin^4\theta_{13}$$

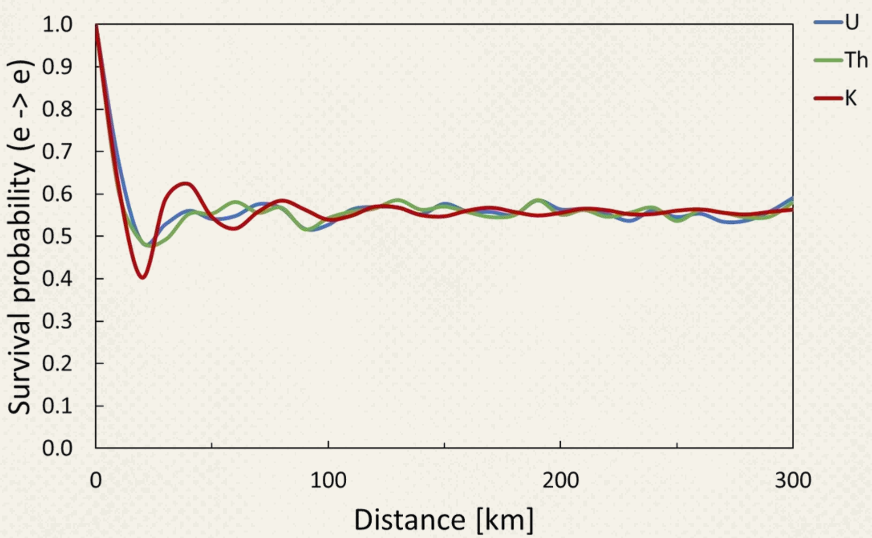

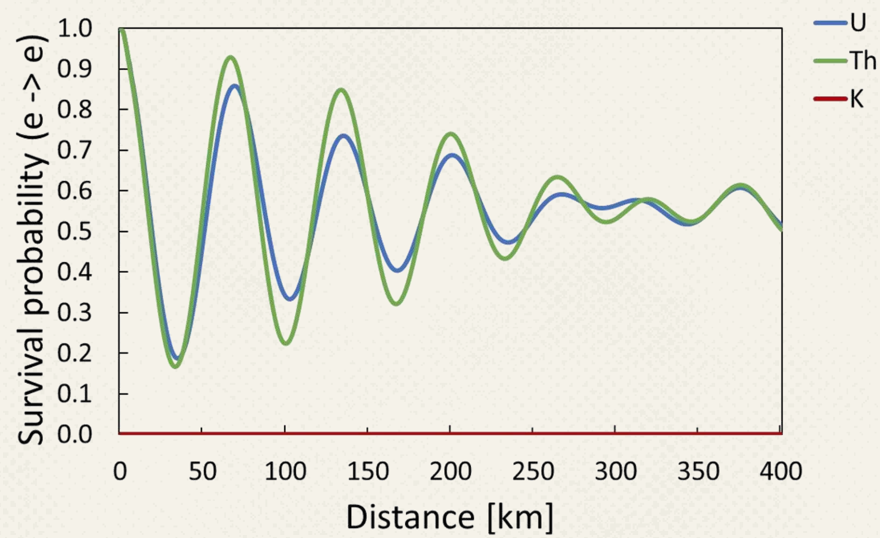

Fermi Function

$$F(Z,E,R) = \frac{|\phi_e(R)_{Coulomb}|^2}{|\phi_e(R)_{Free}|^2} = 2(1+\gamma)(2pR)^{2\gamma-2} e^{\pi\eta} \left|\frac{\Gamma(\gamma+i\eta)}{\Gamma(2\gamma+1)}\right|^2$$

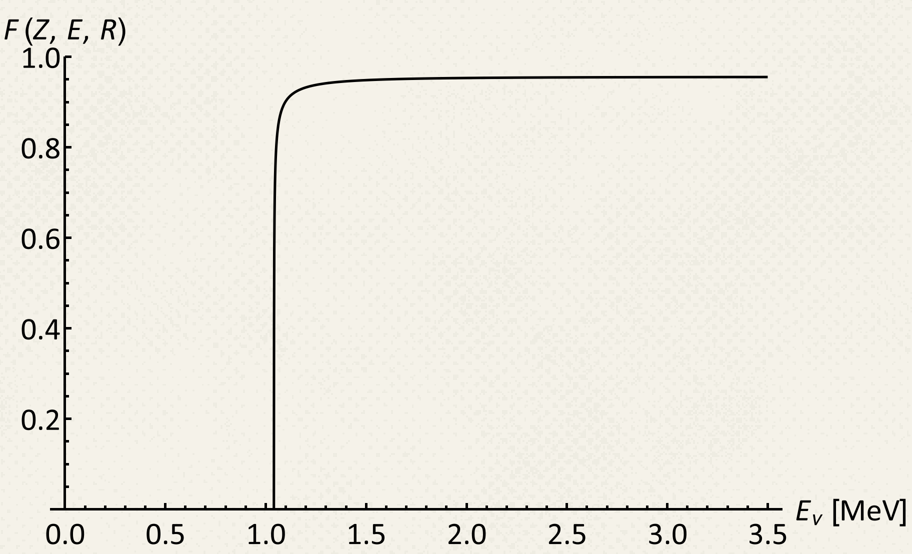

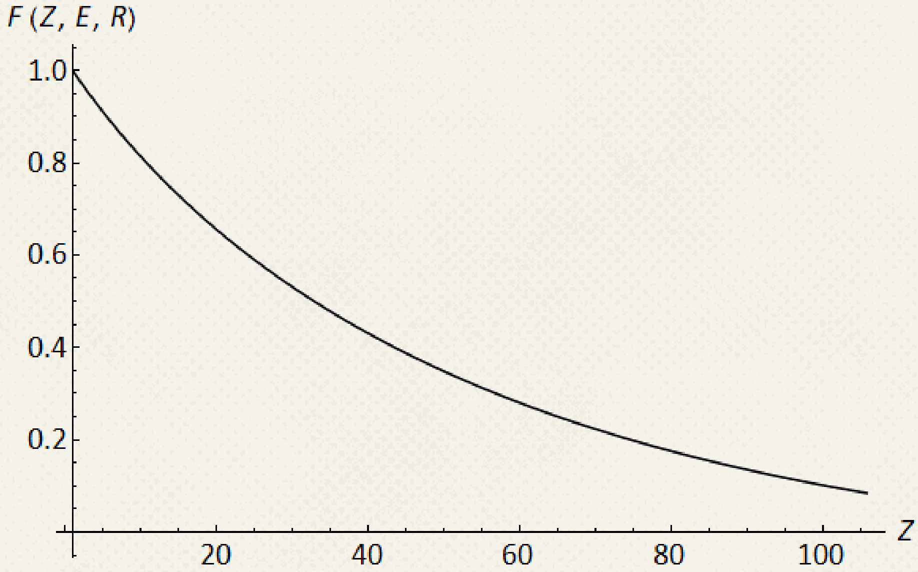

$$\eta = -\frac{\alpha(Z-1)E}{p} \qquad \gamma = \sqrt{1-\alpha^2(Z-1)^2} \qquad \Gamma(z) = \int_0^\infty x^{z-1} e^{-x} dx = (z-1)!$$

Flux Variability

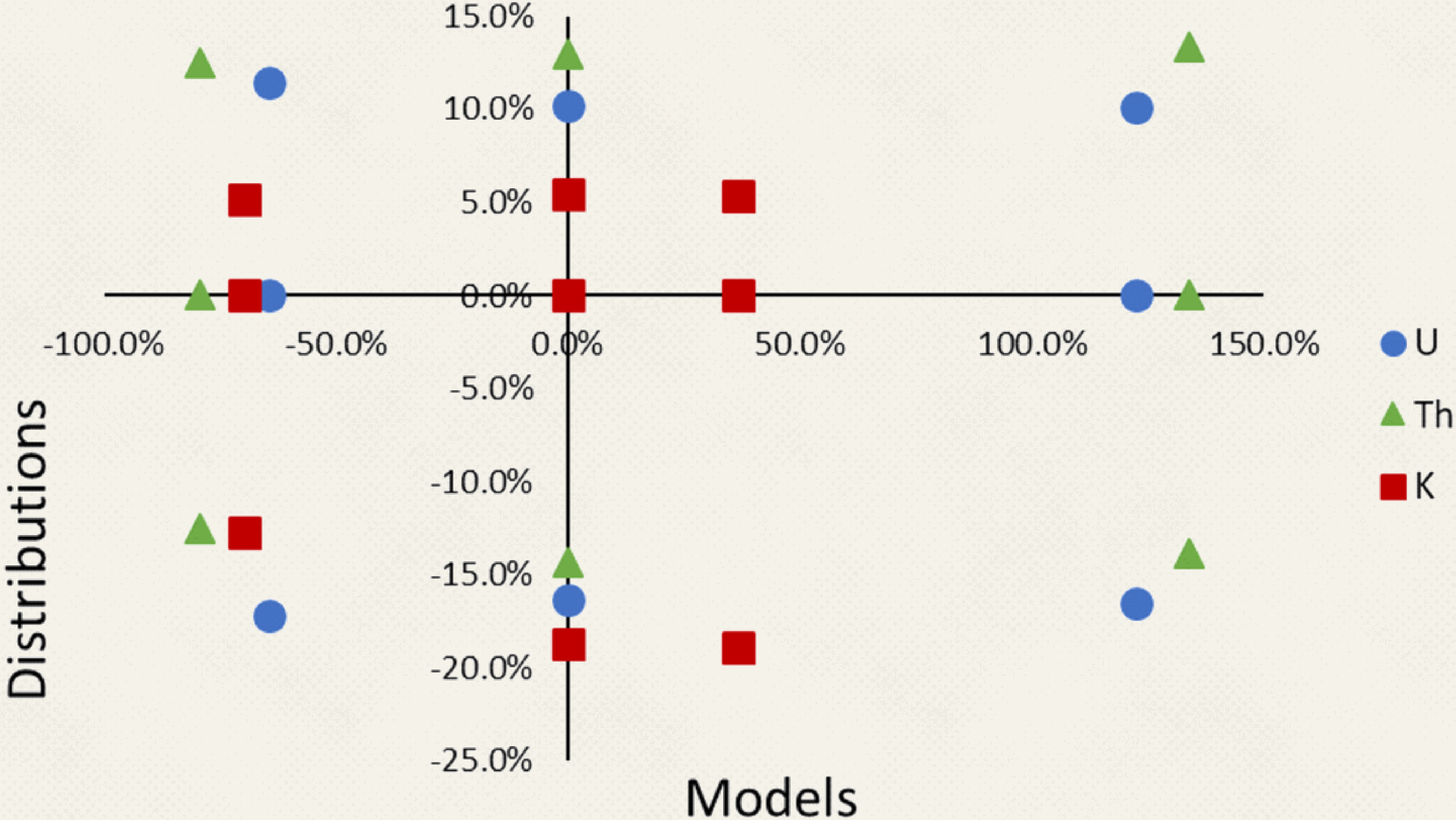

Geo-Dynamo